Discover Public Health

RESEARCH Open Access

Modeling infectious disease dynamics on cruise ships: an enhanced SIR framework with risk index assessment

Ahmed Abdelrazec[1*], Ali Abu-Nada[1], Nathan Kawansson[1], Mostafa Elogail[1] and Saud Aldajah[2]

*Correspondence:
Ahmed Abdelrazec
ahmed.abdelrazec@gmail.com
[1]General Education Department, Sharjah Maritime Academy (SMA), Sharjah, United Arab Emirates
[2]Dean of Applied Studies, Sharjah Maritime Academy (SMA), Sharjah, United Arab Emirates

Abstract

Cruise ships, with their dense populations and constant passenger movement, present highly dynamic conditions for the spread of infectious diseases. Although strict health protocols and monitoring systems are widely implemented, their operational effectiveness often varies. In this study, we develop and analyze an improved Susceptible-Infected-Recovered (SIR) model using early outbreak data to characterize epidemic dynamics in cruise-ship environments. The proposed framework extends the classical SIR model by incorporating ship-specific factors such as transmission rates and confined-space contact structures. Building on this formulation, we introduce a new infection-risk index that quantifies the likelihood of disease transmission and serves as an early indicator of outbreak severity. To evaluate the model's predictive performance and epidemiological relevance, we apply it to empirical data from the MS Voyager COVID-19 outbreak (2021) and an influenza outbreak (2014). Numerical simulations demonstrate that the enhanced model provides more accurate short-term forecasts and facilitates the identification of effective intervention strategies. These results highlight the value of SIR-based modeling approaches for assessing and mitigating epidemic risks in closed, mobile populations such as cruise ships.

Keywords SIR model, Infection risk index, Risk assessment, Infectious diseases, Cruise ships

1 Introduction

Traveling on a cruise ship poses a special and increased risk of infectious disease transmission because of its unique social and physical environments [1]. The frequent social interactions, shared facilities, and close proximity of passengers and crew all contribute to the rapid spread of infectious agents [2]. Additionally, cruise ships act as miniature versions of global mobility, uniting people from various geographical and epidemiological backgrounds who move between several locations in a cramped environment [3]. These characteristics of cruise ships make them ideal to be used as case studies for the creation and verification of infectious disease models that show the dynamics

of transmission in semi-closed populations because of these features [4–6]. A striking example of these dynamics was the outbreak on the Diamond Princess cruise ship during the COVID-19 pandemic. Although strict measures were taken in early stages regarding isolation and quarantine, 19 percent of the 3,711 passengers on board were infected [7]. This is one example of the operational and epidemiological difficulties for efficient containment at sea, which indicates the possibilities of rapid disease amplification in maritime environments [8, 9]. Also, research conducted on cruise ships during outbreaks onboard these ships asserted that airborne transmission through central HVAC systems probably played a role in the spread of the disease outside of direct contact networks [10]. These results highlight the need for improved mathematical models that take into account environmental factors and transmission mechanisms unique to ships. The need for quantitative tools that can support focused health interventions and forecast an outbreak's trajectory in real time is growing in this context. Incorporating dynamic and heterogeneous factors into traditional compartmental frameworks enhances the model's ability to accurately represent the complexities of disease transmission. The SIR model is a compartmental model that is widely used to demonstrate the simulation of population moves from one state to another particularly in modelling infectious diseases [11]. Extensions of the SIR model have been used in cruise ship settings to forecast short-term epidemic trajectories, evaluate the efficacy of interventions, and estimate the basic reproduction number (R_0) [12, 13]. This value was higher in the Diamond Princess incident in comparison to land-based settings, which were explained by the restricted spatial structure and high rates of interpersonal contact [14]. Despite the implementation of existing health protocols such as routine testing, identification and isolation of symptomatic cases, and pre-embarkation screening, the challenge is in ensuring their consistent and efficient execution. The effectiveness of public health interventions may be hampered by elements like restricted medical capacity, inconsistent crew compliance, passenger behavior, and the ship's built environment, including ventilation and airflow systems [15]. Risk assessments play a critical role in this framework, providing a systematic approach to identifying and evaluating the hazards associated with infectious diseases on cruise ships. According to the World Health Organization (WHO), risk assessments involve analyzing the likelihood and consequences of adverse health outcomes, which is essential for developing effective public health strategies [16]. By integrating risk assessments with the SIR model, cruise operators can make informed decisions regarding health protocols and emergency response plans, thereby enhancing the safety of passengers and crew members.

In this study, we integrated the SIR model with risk assessments to presents a comprehensive approach to understanding and managing the risks of infectious diseases on cruise ships. As the industry continues to navigate the challenges posed by infectious diseases, leveraging mathematical modeling and risk assessment will be crucial for safeguarding public health and ensuring the sustainability of cruise operations.

2 Basic SIR model

To investigate the spread of infectious diseases within a cruise ship environment, we begin with the classical Susceptible Infected Recovered (SIR) model. This framework provides a fundamental yet powerful description of epidemic dynamics in a closed

population, where individuals transition sequentially between three mutually exclusive states:

- $S(t)$: the number of *susceptible* individuals who are vulnerable to infection at time t;
- $I(t)$: the number of *infectious* individuals who can transmit the disease at time t; and
- $R(t)$: the number of *recovered* (or removed) individuals who have acquired immunity or are otherwise no longer infectious.

For a cruise ship population, the total number of individuals on board is assumed constant throughout the voyage:

$$N = S(t) + I(t) + R(t). \tag{1}$$

Deaths or disembarkations due to the disease are considered part of the removed group and thus do not alter the total population size. Under these assumptions, the temporal evolution of the epidemic can be expressed as a system of coupled nonlinear differential equations [3]:

$$\frac{dS}{dt} = -\beta SI, \tag{2}$$

$$\frac{dI}{dt} = \beta SI - \alpha I, \tag{3}$$

$$\frac{dR}{dt} = \alpha I. \tag{4}$$

Here, the parameters β and α have the following interpretations:

- β is the *transmission rate* (or contact rate), representing the frequency with which susceptible and infectious individuals interact in a way that leads to infection. Additionally, in this model we assume that the total number of contacts a person has increases proportionally with the population density;
- α is the *recovery rate* (or removal rate), representing the inverse of the average infectious p-eriod.

It is important to note that the SIR equations (Eq. 4) assume a constant population. This assumption is valid for epidemics that develop over a short time frame, allowing us to disregard the effects of deaths and new births. However, new births contribute to the susceptible population, and if the epidemic persists over a longer duration, these factors should be incorporated into the model. This inclusion may result in the emergence of an endemic state.

The ratio between these two parameters defines a characteristic epidemic threshold:

$$\mu = \frac{\alpha}{\beta}. \tag{5}$$

This μ represents the epidemic threshold, the epidemic can develop only if the population is above the epidemic threshold. In other word When $S(t) > \mu$, the number of infected individuals grows; when $S(t) < \mu$, the epidemic declines.

2.1 Integral form and conservation of population

From Eq. (4), we can integrate to obtain:

$$R(t) = R(t_0) + \alpha \int_{t_0}^{t} I(y)\, dy, \tag{6}$$

which relates the cumulative number of recovered individuals to the area under the infection curve. Since the total population N is constant, this integral form provides a useful validation tool for numerical simulations.

2.2 The basic reproduction number R_0

A central quantity in epidemic modeling is the *basic reproduction number*, defined as:

$$R_0 = \frac{S_0}{\mu} = \frac{\beta S_0}{\alpha}, \tag{7}$$

where S_0 is the initial number of susceptible individuals. R_0 represents the average number of secondary infections generated by one infectious individual introduced into a completely susceptible population [17].

If $R_0 > 1$, each infection generates more than one new case, and the epidemic will expand; if $R_0 < 1$, the infection will die out. This threshold is a key measure for assessing the effectiveness of public health interventions [18].

2.3 Relationship between susceptible and infectious populations

Eliminating time from Eqs. (2) and (3), we can derive a direct relationship between $I(t)$ and $S(t)$. Integrating $\frac{dI}{dS} = -1 + \frac{\alpha}{\beta S}$ gives:

$$I = I_0 + (S_0 - S) + \mu \ln\left(\frac{S}{S_0}\right), \tag{8}$$

where I_0 and S_0 are the initial values of $I(t)$ and $S(t)$, respectively; unless there are naturally immune individuals (which is not the case for new infections), $S_0 = N - I_0$. This expression captures how the number of infections evolves as the susceptible population is depleted, then:

$$I = (N - S) + \mu \ln\left(\frac{S}{S_0}\right). \tag{9}$$

From this relationship, we infer that the epidemic reaches its maximum when $S = \mu$, meaning that the fraction of susceptible individuals has declined to the critical threshold required for epidemic decline.

2.4 Parameter sensitivity and containment strategies

To understand the impact of control measures aboard cruise ships, we examine how variations in α and β affect epidemic behavior. These parameters correspond to interventions that influence recovery (e.g., medical isolation, treatment) and transmission (e.g., social distancing, hygiene), respectively. For instance, promptly isolating infected individuals increases the recovery rate α, while reducing social contacts decreases the contact rate β. Both of these actions result in an increase in the epidemic threshold μ. If

μ exceeds the total population N, the epidemic will cease, meaning that the number of infected individuals will begin to decline, although new infections may still occur. Alternatively, the same effect can be achieved by reducing the population N (while keeping β and α constant) by partitioning it into non-communicating compartments, each with a population below the epidemic threshold.

Figure 1 illustrates the temporal evolution of the number of infected individuals, $I(t)$, under different combinations of the transmission rate β and the recovery rate α, while keeping the epidemic threshold $\mu = \alpha/\beta$ constant. The three curves correspond to scenarios where both parameters are scaled proportionally but with different magnitudes of α and β: the solid blue curve represents the baseline case, the dotted red curve a moderate reduction of both rates, and the dashed green curve a stronger reduction.

Although the epidemic threshold μ remains unchanged across the three simulations, the rate at which the infection grows and decays varies substantially. The figure demonstrates that when α and β are reduced simultaneously, the shape of the infection curve stretches along the time axis. In other words, the epidemic unfolds more slowly, with a longer duration but approximately the same total number of cases. The peak infection level (maximum of $I(t)$) remains nearly identical because the balance between transmission and recovery is preserved through the constant μ ratio.

From an epidemiological perspective, this slowing effect is highly significant. It suggests that even without altering the ultimate size of the outbreak, lowering contact frequency (reducing β) together with improved isolation measures (lowering α proportionally to maintain μ) can "flatten the curve," decreasing the instantaneous burden on onboard medical facilities. The cruise ship environment, characterized by limited medical capacity and isolation space, would greatly benefit from this temporal spreading of cases, allowing time for resource allocation, testing, and targeted interventions.

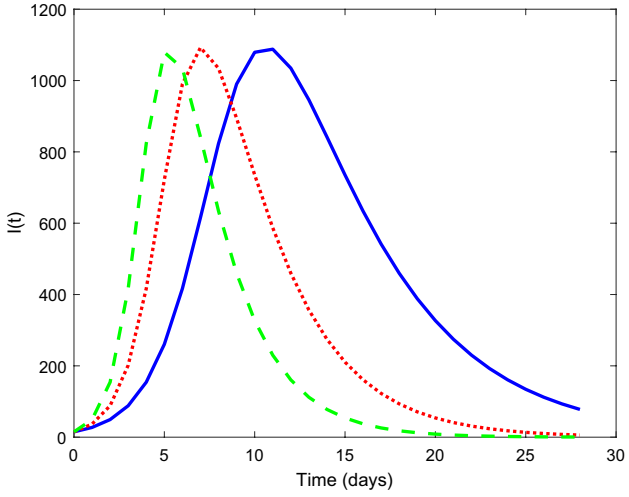

Fig. 1 Temporal evolution of the number of infected individuals $I(t)$ for different proportional changes in the transmission rate (β) and recovery rate (α) while keeping the epidemic threshold $\mu = \alpha/\beta$ constant. the three curves represent distinct time scales of the outbreak: In particular we have considered $S_0 = 3000, I_0 = 10$, and $\alpha = \alpha_0 = 0.1, \beta = \beta_0 = 10^{-3}$ (dashed green curve shows a rapid rise and fall due to higher interaction frequency). In case $\alpha = \alpha_1 = \frac{3\alpha_0}{4}, \beta = \beta_1 = \frac{3\beta_0}{4}$ (dotted red curve depicts a moderately slower spread); and if $\alpha = \alpha_2 = \frac{\alpha_0}{2}, \beta = \beta_2 = \frac{\beta_0}{2}$ the solid blue curve indicates a prolonged but less abrupt progression. Although the total number of infections and the peak magnitude remain nearly identical, lowering both α and β proportionally delays the epidemic, effectively "flattening the curve" and providing more time for containment and medical intervention aboard the cruise ship

Quantitatively, the steeper ascent of the green dashed curve indicates that higher β values accelerate early exponential growth, producing an outbreak that peaks earlier but declines more rapidly as the susceptible pool is exhausted. Conversely, the blue curve (lower β and α) exhibits a slower rise, delayed peak, and prolonged tail, reflecting extended but milder infection dynamics. These results emphasize that modifying both transmission and recovery rates proportionally affects the epidemic's "timescale" rather than its "magnitude".

In practical terms for cruise-ship management, such parameter tuning corresponds to moderate behavioral interventions—such as scheduled dining, staggered activities, or ventilation improvements—that reduce the average contact rate without drastically changing the balance between infection and recovery. The model therefore highlights that the same basic epidemic potential (fixed μ) can yield very different operational outcomes depending on the temporal profile of the outbreak, which directly impacts quarantine logistics and passenger safety planning.

Figure 2 examines how the epidemic dynamics change when the threshold parameter $\mu = \alpha/\beta$ is varied by altering α or β independently. Unlike Fig. 1, where μ was held constant, here we explicitly explore the consequences of shifting the balance between transmission and recovery rates. We will thus choose an arbitrary (but realistic) set of parameters, which should be thought of as being extracted from the time series for the early phase of the epidemic. We consider $S_0 = 2000$, and $I_0 = 10$, with different values of parameters. The red solid line represents the baseline scenario (when we considered $\alpha = 0.1, \beta = 0.001$ and $\mu = 100$), while the dashed and dotted curves correspond to cases where μ decreases or increases, respectively.

When μ is reduced, for instance, by increasing $\beta = 0.0015$ with $\alpha = 0.1$ (more frequent or higher-risk contact; dotted black curve) or decreasing $\alpha = 0.05$ with $\beta = 0.001$ (slower recovery; dashed green curve), the epidemic becomes significantly more

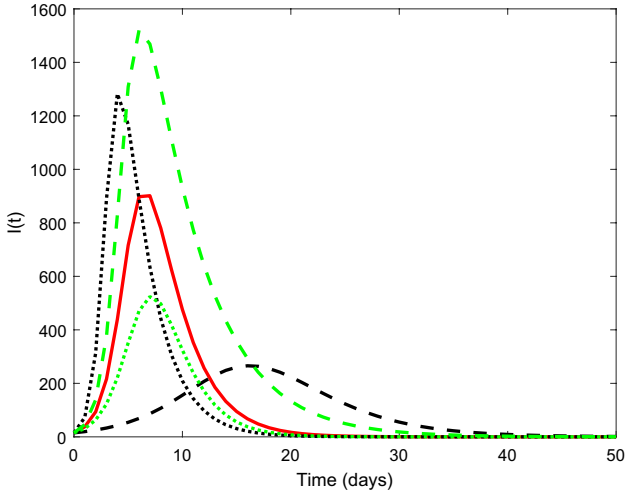

Fig. 2 Temporal evolution of the infection curve $I(t)$ for different values of the epidemic threshold $\mu = \alpha/\beta$. The solid red line represents the baseline scenario, while the dashed and dotted curves correspond to altered ratios of recovery to transmission rates. A smaller μ (green dashed curve), resulting from increased transmission or slower recovery, produces a higher and sharper epidemic peak, indicating faster disease amplification and prolonged persistence. Conversely, larger μ values (black dotted curve) yield flatter and shorter outbreaks due to more effective recovery or reduced contact rates. These results highlight the sensitivity of epidemic severity and duration to small variations in μ, emphasizing the importance of rapid medical response and transmission control in cruise ship environments

aggressive. Both curves showing a steeper rise, a higher infection peak, and a longer decay period. The infection grows rapidly because the reproduction number $R_0 = S_0/\mu$ increases; in epidemiological terms, each infected individual transmits the disease to more secondary cases. Such behavior mirrors conditions aboard cruise ships with limited isolation capacity or insufficient ventilation, where close contact and prolonged exposure lead to faster viral propagation.

Conversely, increasing μ through interventions that either shorten the infectious period (raising $\alpha = 0.5$ with $\beta = 0.001$ via rapid detection, isolation, or effective treatment; dot green curve) or reduce transmission (lowering $\beta = 0.0002$ with $\alpha = 0.1$ through distancing and sanitation; dashed black curve) has a suppressive effect on epidemic growth. Both curves in Fig. 2 demonstrates a slower outbreak with a lower infection peak and shorter duration. These outcomes correspond to improved health-management scenarios on board, where prompt medical response and structured movement protocols limit disease amplification.

The figure also reveals a nonlinear sensitivity of the epidemic trajectory to μ. Small proportional changes in μ can yield disproportionately large differences in both the amplitude and duration of $I(t)$. This property emphasizes that the threshold parameter μ acts as a control lever for outbreak management: small improvements in transmission control or recovery rate can lead to substantial reductions in epidemic burden.

From a public-health operations perspective, these dynamics underscore the importance of maintaining a high effective μ through preventive strategies. On cruise ships, this could involve improving air-filtration systems, scheduling activities to reduce crowd density, and enforcing rapid testing and isolation protocols. As shown in Fig. 2, maintaining μ above the critical threshold can mean the difference between a short, contained outbreak and a prolonged epidemic that overwhelms limited onboard resources.

2.5 Model adaptation for cruise ship populations

Applying the SIR model to cruise ship populations requires specific adjustments due to their limited size and unique social structure. The relatively small, semi-closed nature of cruise ships makes them highly sensitive to stochastic fluctuations and contact heterogeneity. Consequently, purely deterministic predictions may not accurately reflect real-world outbreak behavior.

To address this, adaptive and data-driven extensions of the SIR model can be implemented. By updating model parameters in real time based on daily infection data and accounting for stochastic variability, the model can more accurately predict infection trajectories. Such an approach provides a robust analytical framework for assessing containment strategies, optimizing quarantine protocols, and forecasting outbreak outcomes in maritime environments.

3 A model with risk assessment index

In this section, we introduce a quantitative index designed to evaluate and forecast the risk of infectious disease transmission aboard cruise ships. The index, termed the *Minimum Infection Rate (MIR)*, serves as an early-warning metric that reflects both the current infection status and the effectiveness of ongoing preventive measures. By tracking the MIR over time, health authorities can anticipate short-term epidemic trends, evaluate intervention efficacy, and adjust mitigation strategies accordingly.

3.1 Definition of the minimum infection rate (MIR)

The proposed MIR is defined as:

$$MIR(t) = (1 - a)\frac{I(t)}{N_{\max}}, \tag{10}$$

where, $I(t)$ is the number of infectious individuals at time t, $N_{\max}$ denotes the maximum capacity of the cruise ship, representing the total number of individuals on board, and a is the *preventive efficiency factor*, quantifying the overall effectiveness of implemented preventive measures. The parameter a ranges between 0 and 1. A value of $a = 0$ corresponds to the absence of any preventive measures, while $a = 1$ represents perfect prevention where disease transmission is completely halted. Intermediate values of a reflect partial compliance or imperfect mitigation, capturing the real-world variability of human behavior and operational constraints.

For practical application, a can be estimated from real epidemiological data collected weekly from cruise ship health reports or surveillance systems. This allows MIR to function as a dynamic indicator, continuously updated based on observed conditions. Once initialized with an infectious individual during the first week of the cruise trip, we can calculate the value of a as the ratio of the average number of recovery with preventive measures to the average number of infections during that week, and then simulate our model for the entire period using 1-day time step for one week. This is repeated weekly while updating the total number of infected human.

In other wards, a values of a are changed from week t_i to week t_{i+1} but are considered constant in the intervals $[t_i, t_{i+1})$. Thus, in the intervals $[t_i, t_{i+1})$ the time variation of the MIR can be derived by differentiating Eq. (16), which is $\frac{d(MIR)}{dt} = \frac{(1-a))}{N_{\max}}\frac{dI(t)}{dt}$. From Eq. (3) we can conclude that:

$$\frac{d\,(MIR)}{dt} = (\beta S - \alpha)MIR. \tag{11}$$

Substituting the relation $\mu = \frac{\alpha}{\beta}$ and $R_0(t) = \frac{S(t)}{\mu}$ from Eq. (7), the equation (11) becomes:

$$\frac{dMIR}{dt} = \beta\mu[R_0(t) - 1]MIR. \tag{12}$$

Equation (12) reveals that the rate of change of the MIR depends directly on the instantaneous reproduction number $R_0(t)$. When $R_0(t) > 1$, the MIR increases, indicating an expanding epidemic; when $R_0(t) < 1$, it declines, signaling effective containment.

3.2 Integration of MIR into the SIR framework

In the intervals $[t_i, t_{i+1})$, to embed MIR risk measure into the epidemic model, we extend the traditional SIR system to include the MIR as an auxiliary variable:

$$\frac{dS}{dt} = -\beta SI, \tag{13}$$

$$\frac{dI}{dt} = \beta SI - \alpha I, \tag{14}$$

$$\frac{dR}{dt} = \alpha I, \tag{15}$$

$$MIR(t) = (1-a)\frac{I}{N_{\max}}. \tag{16}$$

Here, the standard SIR dynamics remain valid, but the MIR provides an interpretable link between model variables and the real-world risk of infection spread. This coupling allows for a more actionable representation of the epidemic, where changes in the MIR can directly inform decisions about testing, isolation, and social-distancing protocols on board.

The tool utilizes the MIR, allowing operators or health officials to collect data on the number of recoveries and infected individuals after the first week of the cruise. They can then estimate the parameters α, β and a, along with the initial values. By simulating the model, they can predict the risk of infection for the upcoming week by calculating the value of MIR. Based on the MIR value, appropriate actions or policies can be implemented, such as requiring masks, creating distance between passengers, or reducing contact rates. This strategy can be repeated each week until the end of the trip.

3.3 Interpretation and epidemiological implications

The MIR thus acts as a proxy for the epidemic growth potential at any given time. Because $MIR(t)$ is proportional to $I(t)$ but scaled by both ship capacity and prevention efficiency, it provides a normalized measure of infection risk that can be compared across different voyages, ship sizes, or intervention strategies.

As noted by Roberts [19], an infection becomes endemic when $R_0 > 1$, meaning that each infected person generates, on average, more than one secondary case. Within the MIR framework, this condition translates to a positive $\frac{dMIR}{dt}$, or a rising infection risk. Conversely, $R_0 < 1$ corresponds to a negative $\frac{dMIR}{dt}$, indicating a decline in active infection pressure.

In operational terms, monitoring weekly MIR trends can provide cruise ship health officers with real-time feedback on intervention performance. A sudden increase in MIR, for instance, may suggest lapses in compliance with preventive protocols (e.g., mask wearing, ventilation management, or isolation speed), whereas a consistent downward trend would confirm that implemented measures are effective. Hence, MIR serves as both a diagnostic and predictive tool, quantifying ongoing risk and forecasting the short-term infection trajectory.

Furthermore, since a can vary over discrete time intervals (e.g., between successive weeks t_i and t_{i+1}), it is treated as piecewise constant within each period, $a(t) = a_i, \quad t \in [t_i, t_{i+1}]$, allowing for practical recalibration as new data become available. This modular structure ensures that MIR-based predictions remain adaptive and responsive to changing shipboard conditions.

4 Numerical simulation

The extended SIR model incorporating the Minimum Infection Rate (MIR) index, given in Eqs. (13)–(16), was implemented numerically using MATLAB. A uniform time step of one day was adopted to capture the daily variations in infection dynamics throughout the voyage period. The simulation covers the entire duration of a typical cruise,

beginning on the first day of the trip (t_0) and continuing until the last recorded day (t_1). All parameters in the model were assumed constant within each simulation run to facilitate direct comparison with real-world epidemiological data.

4.1 Initial conditions and parameter estimation

Two separate simulation scenarios were analyzed, corresponding to different infectious disease outbreaks recorded on cruise ships:

1. **COVID-19 outbreak (MS *Voyager*, 2021):** The initial number of infectious individuals was set to $I_0 = 1$, while the initial susceptible population was $S_0 = 2650$. The maximum ship capacity was taken as $N_{\max} = 3000$. The value of a initially calculated as $a = 0.712$.
2. **Influenza outbreak (2014):** For comparison, an earlier influenza epidemic on a cruise ship was simulated using $S_0 = 2500$, $I_0 = 1$, and $N_{\max} = 2800$. The value of a initially calculated as $a = 0.6955$.

In both cases, the recovered population at the start of the voyage was assumed negligible ($R(0) = 0$), consistent with the early phase of an onboard outbreak.

The removal rate α was estimated as the reciprocal of the mean recovery or isolation time, obtained from available clinical or observational data (typically 5–10 days for influenza and 10–14 days for COVID-19). The transmission rate β was estimated retrospectively by adjusting model outputs to match observed infection trajectories at $t = 0$, ensuring that the initial growth rate of $I(t)$ aligned with empirical trends.

4.2 Model implementation and data updating

The simulation proceeded iteratively using the Euler forward method. At each daily step, $S > 0$, $I > 0$, and $R > 0$ were updated according to Eqs. (13)–(15), which were implemented numerically, and the MIR value was subsequently calculated using Eq. (16), to quantify the normalized infection risk at that time:

$$MIR(t) = (1 - a)\frac{I(t)}{N_{\max}}, \tag{17}$$

where the parameter a (preventive efficiency) was treated as piecewise constant and updated weekly to reflect operational changes in health measures, such as the introduction of new screening protocols or restrictions on gatherings.

For each simulated week, the model outputs were validated against real infection data obtained from ship health records. The susceptible population was recalculated weekly using:

$$S(t) = N - I(t) - R(t), \tag{18}$$

which ensured consistency between the model and observed cumulative infection counts.

4.3 Results and analysis

Figure 3 compares the time evolution of the computed MIR (normalized infection risk) with the recorded number of infected individuals for both case studies. The results show a clear proportional relationship between MIR and the observed infection counts.

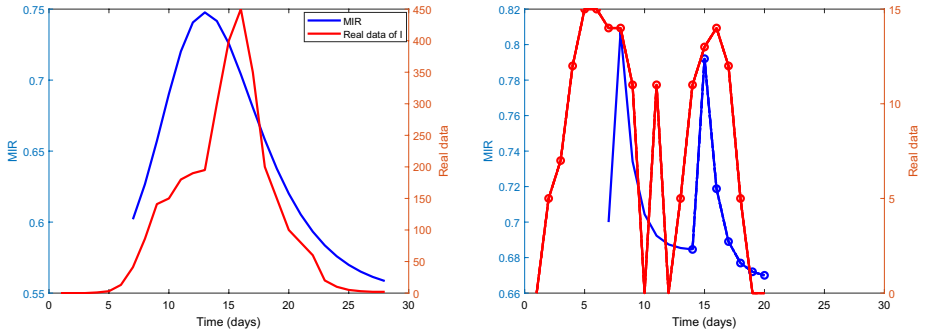

Fig. 3 Comparison between the simulated Minimum Infection Rate (MIR) and the actual number of infected individuals on board. (Left) COVID-19 epidemic on MS *Voyager* (2021). (Right) Influenza outbreak on a cruise ship (2014). The close agreement between MIR predictions and real data validates the proposed index as a dynamic risk-assessment tool

In both outbreaks, the peaks in MIR closely coincide with the maximum number of infected individuals, demonstrating that MIR effectively captures the timing and intensity of infection surges.

For the COVID-19 simulation, the MIR reached its maximum approximately midway through the voyage, consistent with empirical reports from the MS *Voyager* outbreak. This pattern reflects the buildup of infection pressure during the initial phase, followed by a rapid decline once containment measures (e.g., cabin isolation and disembarkation quarantine) were enforced.

The influenza simulation exhibited a similar trend but with a narrower and lower peak, corresponding to a faster natural recovery rate (α) and lower transmission efficiency (β). Despite differences in disease characteristics [20], the MIR consistently mirrored the shape and magnitude of real infection data, confirming its validity as a robust indicator of epidemic intensity.

The proportionality between MIR and ($I(t)$) indicates that MIR not only reflects the ongoing infection burden but also provides early insights into how preventive measures can modify transmission dynamics. As demonstrated in the simulations, increasing a (which represents stricter preventive measures) directly reduces the amplitude of MIR and delays the peak of infections to later times. This predictive capability makes MIR a valuable operational metric for assessing the short-term risk level aboard ships with limited medical infrastructure.

Furthermore, since we assume a remains constant during the simulation and updated weekly, the value of MIR is directly proportional to the infected population. This relationship indicates that MIR serves as a reliable indicator of the risk of infection.

Moreover, the temporal alignment between MIR peaks and actual infection peaks suggests that MIR can be used as a leading indicator for outbreak forecasting. Health authorities can use rising MIR values as a signal to strengthen interventions before infections reach their maximum level, enabling proactive rather than reactive control of onboard epidemics.

Overall, the numerical simulations confirm that integrating MIR into the SIR framework provides an accurate and interpretable model for real-time epidemic assessment in cruise ship settings. By validating the model against COVID-19 and influenza datasets, we demonstrate its generality and adaptability to different pathogens. The MIR-based

model thus offers a valuable analytical and operational tool for epidemic prediction, monitoring, and response in maritime environments.

Acknowledgements
The authors would like to express their sincere gratitude to the Sharjah Maritime Academy for their support in this research.

Author contributions
All authors have the same contribution.

Data availability
The data supporting of this study will be available from the corresponding author as requested.

Declarations

Ethics approval and consent to participate
The research presented in this manuscript adheres to the highest ethical standards. This study was conducted in accordance with ethical guidelines and received approval from the Institutional Review Board of the Sharjah Maritime Academy (SMA). The protocol was approved in accordance with the Key policies include academic integrity rules (https://www.sma.ac.ae/). The work is original, and any ideas or quotations from other sources are properly cited. . Informed consent was obtained from all participants involved in the study. Participants received detailed information about the purpose, procedures, potential risks and benefits of the study and had the opportunity to ask questions before consenting to participate.

Consent for publication
All authors have given their consent for the publication of this manuscript. In addition, participants have been informed that their data may be published and have consented to the use of their data for this purpose.

Competing interests
The authors declare no competing interest and confirm that the mathematical models, data, and results are accurate.

Received: 31 January 2026 / Accepted: 30 July 2026
Published online: 16 August 2026

References

1. Gonzalez E, et al. Covid-19 outbreak on the diamond princess cruise ship. N Engl J Med. 2020;382(6):590–2.
2. Mouchtouri A, Verykouki E, Zamfir E. Transmission of sars-cov-2 associated with cruise ship travel: a systematic review. Trop Med Infect Dis. 2022;7(10):290.
3. Anderson M, May RM. Infectious diseases of humans: dynamics and control. Oxford: Oxford University Press; 1992.
4. Rocklöv J, Sjödin H, Wilder-Smith A. Covid-19 outbreak on the diamond princess cruise ship: estimating the epidemic potential and effectiveness of public health countermeasures. J Travel Med. 2020;27(3):30.
5. Kretzschmar E, et al. Modeling the effectiveness of vaccination and quarantine on containing covid-19 outbreaks in cruise ships. BMC Infect Dis. 2021;21(1):1–10.
6. Khan NN, Begum SA. Vaccine efficacy of covid-19 in bangladesh: Does vaccination prevent the pandemic? J Bangl Math Soc. 2023;43(1):045–62.
7. Expert Taskforce for the COVID-19 Cruise Ship Outbreak. Epidemiology of covid-19 outbreak on cruise ship quarantined at yokohama, japan. Emerg Infect Dis. 2020;26(11):2591–7.
8. Smith D, et al. Evaluating infectious disease outbreak potential and mitigation effectiveness on cruise ships. PLoS ONE. 2023;18(5):e0286203.
9. Koo R. Contact tracing and isolation of cases associated with covid-19 outbreak on the diamond princess cruise ship. J Travel Med. 2020;27(3).
10. Li Y, Qian H, Hang J. Evidence for probable aerosol transmission of sars-cov-2 in a poorly ventilated restaurant. Build Environ. 2021;196:107788.
11. Kermack WO, McKendrick AG. A contribution to the mathematical theory of epidemics. Proc R Soc A. 1927;115(772):700–21.
12. Zhuang Z, Huang X, Li L. How many infections of covid-19 there will be in the "diamond princess" predicted by a virus transmission model based on simulation of crowd flow. 2020.
13. Mohammad K, Akhi A, Kamrujjaman M. Seasonal variability and stochastic branching process in malaria outbreak probability. Acta Trop. 2024;257:107311.
14. Almilaji O. Air recirculation role in the spread of covid-19 onboard the diamond princess cruise ship during a quarantine period. Aerosol Air Qual Res. 2021;21(3):200–495.
15. Centers for Disease Control and Prevention (CDC). Interim guidance for cruise ships during the covid-19 pandemic. https://www.cdc.gov/. 2021.
16. Risk Assessment and Management of Foodborne Diseases. World Health Organization. Geneva, Switzerland; 2017 (World Health Organization (WHO)).
17. Diekmann O, Heesterbeek P, Metz J. On the definition and the computation of the basic reproduction ratio r_0 in models for infectious diseases in heterogeneous populations. J Math Biol. 1990;28:356–82.
18. Heesterbeek JAP. A brief history of r0 and a recipe for its calculation. Acta Biotheor. 2022;50:189–204.
19. Roberts M. The pluses and minuses of r_0. J R Soc Interface. 2007;4(16):949–61.

20. Mohammad KM, Khan T, Kamrujjaman M. Stochastic control of influenza spread: a levy-driven sde and branching process approach. Infect Dis Model. 2026;11.

Publisher's Note